

## Global optical potential for $\alpha$ particles with energies above 80 MeV

M. Nolte, H. Machner, and J. Bojowald

*Institut für Kernphysik, Kernforschungsanlage Jülich, D-5170 Jülich, Federal Republic of Germany*

(Received 25 September 1986; revised manuscript received 4 May 1987)

A set of parameters has been derived for a global optical potential from elastic  $\alpha$ -nucleus scattering with energies higher than 80 MeV. The geometry and energy dependence derived by Put and Paans was adopted. The optical model predictions were tested with data from elastic as well as from inelastic scattering.

### I. INTRODUCTION

The study of  $\alpha$ -particle scattering was proven to be a sensitive tool for studying nuclear matter distributions and transition densities.<sup>1</sup> One reason for this is the fact that the  $\alpha$  particle is a very symmetric nucleus with a simple underlying structure, and therefore there is hope of learning something at the interface between nucleon-nucleus interactions and nucleus-nucleus interactions. As in the nucleon-nucleus case, one would like to express the  $\alpha$ -nucleus interaction in terms of an optical potential. However, low-energy data suffer from discrete and continuous ambiguities in the optical model parameters.<sup>1</sup> One attempt to solve these problems was the adoption of a form factor different from the one employed in the nucleon-nucleus case. There, the data were nicely reproduced by assuming that the density and the potential have the same shape.<sup>2</sup> The folding model analysis suggests a shape more like the square of a Woods-Saxon form factor.<sup>3</sup> However, medium energy data were equally well reproduced by a single Woods-Saxon form factor as by a squared Woods-Saxon form factor.<sup>4</sup> We have tried to derive a global optical potential for the  $\alpha$ -nucleus interaction by only employing a Woods-Saxon form factor.

### II. THE OPTICAL POTENTIAL

The standard optical potential reduces, in the case of  $\alpha$ -nucleus interactions, to

$$U(r) = -Vf(r) - iWg(r) + V_{\text{Coul}}, \quad (1)$$

with form factors of the Woods-Saxon type

$$f(r) = \{1 + \exp[(r - r_v A^{1/3})/a_v]\}^{-1} \quad (2)$$

and

$$g(r) = \{1 + \exp[(r - r_w A^{1/3})/a_w]\}^{-1}; \quad (3)$$

$V_{\text{Coul}}$  denotes the Coulomb potential. In this description the potential is determined by six parameters. It was found, by Singh *et al.* (Ref. 5) and by Put and Paans (Ref. 6), that the radius parameters  $r_{v,w}$  and the diffuseness parameters  $a_{v,w}$  are rather constant for  $\alpha$ -particle energies above 80 MeV. We, therefore, chose a

fixed geometry and allowed only the real potential depth  $V$  and the imaginary potential depth  $W$  to vary with the energy and target mass number. For simplicity we adopted, as a first choice, the values for  $a_{v,w}$  and  $r_{v,w}$  derived by Put and Paans from a study of elastic  $\alpha$ -particle scattering on  $^{90}\text{Zr}$ ;<sup>6</sup>

$$\begin{aligned} r_v &= 1.245 \text{ fm}, \\ a_v &= 0.801 \text{ fm}, \\ r_w &= 1.570 \text{ fm}, \end{aligned} \quad (4)$$

and

$$a_w = 0.567 \text{ fm}.$$

We furthermore adopted the energy dependence for  $V$  and  $W$  found in that work,

$$V(E_\alpha) = V_0(1 + \alpha_v E_\alpha), \quad (5)$$

with  $V_0(^{90}\text{Zr}) = 155.2 \text{ MeV}$  and  $\alpha_v(^{90}\text{Zr}) = -0.0016 \text{ MeV}^{-1}$  and similarly for  $W$ ,

$$W_0(^{90}\text{Zr}) = 19.17 \text{ MeV} \quad \text{and} \quad \alpha_w(^{90}\text{Zr}) = 0.0003 \text{ MeV}^{-1}.$$

We wanted to derive an expression for the potential depths in the form

$$V(A, Z, E_\alpha) = a_0 + a_1 Z A^{-1/3} + a_2 E_\alpha \quad (6)$$

and

$$W(A, E_\alpha) = b_0 + b_1 A^{1/3} + b_2 E_\alpha. \quad (7)$$

The dependences of the real potential depth [Eq. (6)] were similar to those introduced by Perey for nucleons.<sup>7</sup> The symmetry potential necessary to describe nucleon-nucleus scattering is not effective in the case of  $\alpha$ -particle scattering. The term proportional to  $Z/A^{1/3}$  was introduced by Perey<sup>7</sup> as a correction for effects introduced by Coulomb repulsion. The average Coulomb potential at the nuclear surface is proportional to  $Z/R$  and hence proportional to  $Z/A^{1/3}$ . The imaginary potential depth in the case of nucleons showed no mass dependence.<sup>2,7</sup> However, for deuteron scattering a linear dependence of the imaginary potential on the nuclear radius has been observed<sup>8</sup> and is therefore also assumed in

TABLE I. Derived optical model depths for 140 MeV  $\alpha$ -particle scattering on the indicated target nuclei. The geometry parameters are those in Ref. 6. The total absorption cross sections are also given. For details see text.

Nucleus	$V$ (MeV)	$W$ (MeV)	$\chi^2/N$ (best fit)	$\sigma_r(b)$	Ref.	$\chi^2/N$ (global potential)
$^{12}\text{C}$	91.5	31.5	13.4	0.77	10	14.1
$^{40}\text{Ca}$	122.5	27.8	4.8	1.37	10	18.9
$^{50}\text{Ti}$	123.0	24.9	2.8	1.52	9	16.2
$^{58}\text{Ni}$	115.0	21.3	0.8	1.58	10	6.6
$^{90}\text{Zr}$	122.8	20.4	0.62	1.97	10	9.3

TABLE II. Deduced parameters  $a$  and  $b$  for the potential depths [Eqs. (5) and (6)].

Real potential		Imaginary potential	
$a_0$ (MeV)	$116.1 \pm 18.9$	$b_0$ (MeV)	$43.67 \pm 17.19$
$a_1$ (MeV)	$4.77 \pm 1.62$	$b_1$ (MeV)	$-5.55 \pm 1.23$
$a_2$	$-0.248 \pm 0.047$	$b_2$	$0.006 \pm 0.012$

TABLE III. Same as Table I but with four potential parameters constrained.

Nucleus	$V$ (MeV)	$W$ (MeV)	$a_v$ (fm)	$a_w$ (fm)	$\chi^2/N$ (best fit)	$\sigma_r$ (b)	Ref.	$\chi^2/N$ (Global potential)
$^{12}\text{C}$	89.5	23.5	0.751	0.651	5.57	0.77	10	20.1
$^{40}\text{Ca}$	109.7	21.8	0.818	0.684	0.25	1.43	10	12.6
$^{50}\text{Ti}$	114.1	21.8	0.802	0.628	0.42	1.55	9	11.7
$^{58}\text{Ni}$	116.2	21.7	0.792	0.549	0.57	1.56	10	6.8
$^{90}\text{Zr}$	123.1	20.4	0.806	0.562	1.66	1.97	10	7.1
$^{208}\text{Pb}$	159.4	17.2	0.733	0.607	65.9	2.98	12	82.7

TABLE IV. Global potential parameters [Eqs. (6)–(9)] with four parameters constrained.

$a_0$ (MeV)	$101.1 \pm 28.3$
$a_1$ (MeV)	$6.051 \pm 0.373$
$a_2$	$-0.248 \pm 0.047$
$b_0$ (MeV)	$26.82 \pm 75.98$
$b_1$ (MeV)	$-1.706 \pm 0.182$
$b_2$	$0.006 \pm 0.012$
$c_0$ (MeV)	$0.817 \pm 0.053$
$c_1$ (MeV)	$-0.0085 \pm 0.013$
$d_0$ (MeV)	$0.692 \pm 0.076$
$d_1$ (MeV)	$-0.020 \pm 0.019$

TABLE V. Results of the present global optical potential (Table II) for elastic  $\alpha$ -particle scattering on  $^{58}\text{Ni}$ .

$E_\alpha$ (MeV)	$\sigma_r$ (b)	$\chi^2/N$	Ref.
29	1.47	31.7	19
38	1.56	99.4	19
58	1.62	97.1	19
104	1.63	18.8	20
141.5	1.60	6.6	12
172.5	1.57	8.2	4

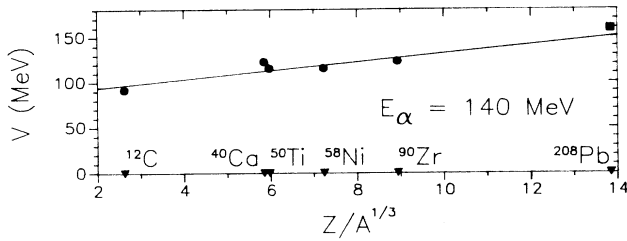


FIG. 1. Mass number dependence of the real potential depth at  $E_\alpha = 140$  MeV. The regression line is also shown. The value for  $^{208}\text{Pb}$  (square) was excluded in the present analysis because of the large  $\chi^2$  value obtained in the fit.

Eq. (7).

The parameters  $a_{0,1}$  and  $b_{0,1}$  are easily derived if data with different mass numbers but constant  $\alpha$ -particle energy are fitted. We have performed such a task from the data sets of Refs. 9 and 10 for target mass numbers spanning the periodic table and at an  $\alpha$ -particle energy of 140 MeV. Because no errors from the experimental results were given in most papers we assumed, for all analyses presented in the present work, an uncertainty of 10%. A two parameter search—namely for  $V$  and  $W$ —was done by employing the optical model code MAGALI.<sup>11</sup> The resulting potential depths are given in Table I. Similar to Ref. 12 we were unable to fit the large angle data in the case of  $^{208}\text{Pb}$ . Therefore, the analysis is restricted to mass numbers only up to  $^{90}\text{Zr}$ . By the inspection of the  $\chi^2$  values (per degree of freedom) given in Table I, one finds that this number increases with decreasing mass number. Obviously, this is a hint that the adopted geometry or the energy dependence of the potential worsens the more the target nucleus differs in mass from  $^{90}\text{Zr}$ . However, in the Ni region the  $\chi^2$  value achieved is still comparable with those from six parameter searches.<sup>4,13</sup>

The mass number dependences are also shown in Figs. 1 and 2 together with regression curves. The resulting parameters are given in Table II. The errors given for the energy dependence are those of Put and Paans, while those of the  $A$  dependence are from the fit of the line to the points shown in Figs. 1 and 2. If we apply the present global potential, i.e., without  $V$  and  $W$  being

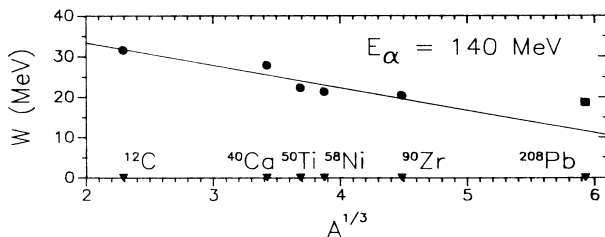


FIG. 2. Same as Fig. 1, but for the imaginary part.

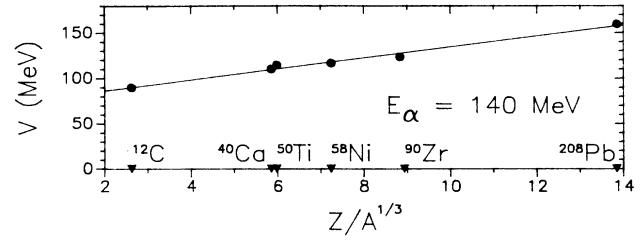


FIG. 3. Same as Fig. 1, but for four constrained parameters.

constrained, to the same data we still achieve satisfactory reproduction of the data. The  $\chi^2$  values are, however, increased considerably (see Table I).

As already mentioned above, it may be that a two parameter search is not adequate for a large mass interval. We, therefore, have repeated the analysis by also assuming an  $A$  dependence of the diffuseness parameters:

$$a_v = c_0 + c_1 A^{1/3} \quad (8)$$

and

$$a_w = d_0 + d_1 A^{1/3} \quad (9)$$

The resulting mass number dependences of the potential depths are similar as before (see Figs. 3 and 4). The mass number dependence of the real diffuseness parameter is weak and nearly a constant up to  $A = 90$ . However, the values for the scattering on lead call for a small mass number dependence. The dependence of  $a_w$  on  $A$  is slightly larger (Fig. 5). The results of the four parameter fits are given in Table III. The quality of the fits is superior compared to the two parameter fits given in Table I. The fit for  $^{208}\text{Pb}$  is improved but still not very satisfactory. The derived  $\chi^2$  values for the global potential parameters Eqs. (6–9) given in Table IV are also shown in Table III. They are close to those values obtained with the global potential parameters employing constant  $a$  values. We will therefore stick in the following to the simpler approach.

### III. DISCUSSION

We have derived for the first time—to the best of our knowledge—a “global”  $\alpha$ -nucleus potential with the

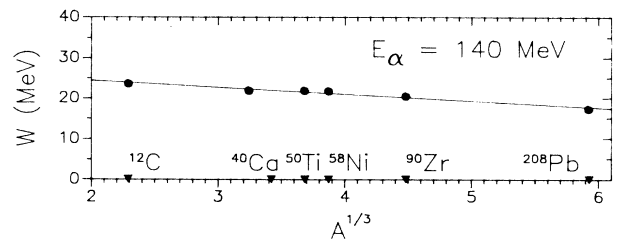


FIG. 4. Same as Fig. 3, but for the imaginary part.

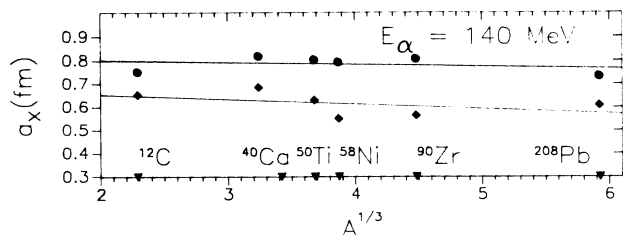


FIG. 5. Mass number dependences of the diffuseness parameters  $a_x$  in four parameter fits. The results for  $x=v$  are shown as dots, those for  $x=w$  as diamonds. Also shown are linear fits to the data with fit parameters given in Table IV.

Woods-Saxon form factors. Since we are interested in medium energies where the geometry becomes independent of energy (the so called Put-Paans effect) we could neglect the explicit treatment of the surface absorption. The Put-Paans geometry valid for  $^{90}\text{Zr}$  seems to depend only weakly on the target mass number. This becomes obvious by comparing these values with those derived in Ref. 5.

The mass dependence found here for both the real part as well as the imaginary part of the potential is much stronger than those for nucleon-nucleus potentials.<sup>14</sup> The imaginary part seems to be almost independent of the energy. Since global optical potential parameters for light composite projectile particles are scarce, comparisons with those suffer from different energy ranges. For low energies and in the case of neutrons and protons Becchetti and Greenlees<sup>2</sup> give a rather strong energy dependence, even stronger than for the real part. Bojowald *et al.* (Ref. 8) report, for low energy deuterons, an energy independent optical potential whereas for energies above 22.5 MeV/nucleon it becomes energy dependent. To check the derived energy dependences for target nuclei different from  $^{90}\text{Zr}$  the volume integrals for the real part as well as the imaginary part of the present potential were compared with the systematics of Motoba *et al.* (Ref. 15). They nicely agree with these systematics. However, this is also true for small energies

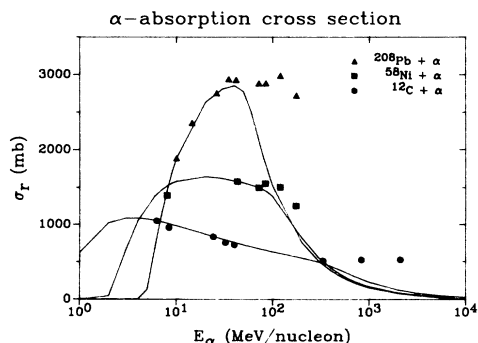


FIG. 6. Total absorption cross sections for the indicated reactions. The data are from Ref. 16. The present optical model predictions are shown as solid curves.

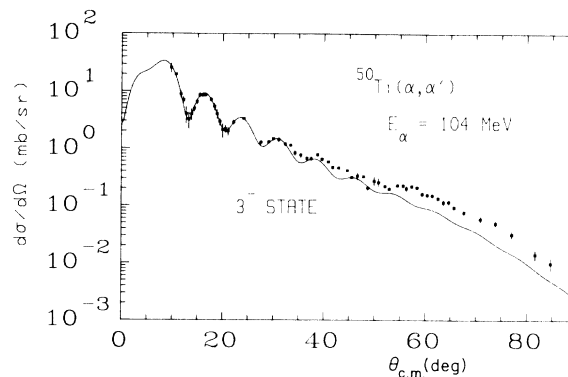


FIG. 7. Measured (Ref. 17) and with the present optical model calculated cross sections for the first  $3^-$  state in  $^{50}\text{Ti}$ . For details see text.

where the present potential, because of its geometry, fails to reproduce elastic scattering data.

A test of the potential, which is in some respect similar to volume integral comparison, is to look at the predictions for total reaction cross sections. Such a comparison is shown in Fig. 6. The data for the different target nuclei are from Ref. 16. These data are reproduced from small energies up to 200 MeV/nucleon for light and medium heavy nuclei whereas for heavy nuclei, agreement is achieved up to 80 MeV/nucleon. This is a much broader range of energies than that where the potential is expected to work and, as already said above, it does not work at low energies.

More stringent tests are needed. To check the mass dependence of the parameter set at a different energy, elastic scattering data taken at 104 MeV by the Karlsruhe group<sup>17</sup> were compared with the present potential predictions. These data are nicely reproduced. To test the energy dependence at a mass number different from  $^{90}\text{Zr}$ , elastic scattering data on  $^{58}\text{Ni}$  with bombarding energies ranging from 29 MeV up to 172.5 MeV (Refs. 4, 12, 19, and 20) were compared with the present optical model predictions. In a few cases no data were available to us. In these cases we took equidistant points obtained by employing the best fit parameters given in the literature (Refs. 12 and 20). The obtained  $\chi^2$  values are given in Table V. As already observed by Put and Paans<sup>6</sup> in the case of  $^{90}\text{Zr}$ , it is impossible to reproduce low energy data with an energy independent geometry. At higher  $\alpha$ -particle energies we achieve a very good reproduction of the data. Another test of the present optical model is its ability to account for inelastic scattering data. For that purpose not too low lying states were chosen where channel coupling is expected to be small. Calculations were performed within the distorted-wave Born approximation (DWBA) using the code DWUCK IV.<sup>18</sup> These tests again give satisfactory results thus giving confidence in the validity of the present parameter set. An example is shown in Fig. 7 for the first  $3^-$  state at  $E_{ex} = 4.42$  MeV in  $^{50}\text{Ti}$ . The

data of Ref. 17 are reproduced by fitting a deformation parameter  $\beta_3=0.17$  employing a Woods-Saxon derivative as form factor. This must be compared with the value given in Ref. 17 obtained in a coupled channel analysis,  $\beta_3=0.133$ . It can therefore be concluded that we have derived a set of parameters for a global  $\alpha$ -nucleus optical potential. This potential is able to reproduce cross sections from elastic, as well as inelastic

scattering for energies above 80 MeV and light to medium heavy nuclei. It fails at backward angles in the case of  $^{208}\text{Pb}$ , as has been the case for so called best fit searches.<sup>12</sup>

We gratefully acknowledge discussions with Prof. H. Rebel and Prof. H. J. Gils. One of us (H.M.) is grateful to Prof. Budzanowski for stimulating discussions.

- <sup>1</sup>*Proceedings of the 2nd Louvain-Cracow Seminar on the Alpha-Nucleus Interaction*, Louvain-la-Neuve, 1978, edited by G. Gregoire and K. Grotowski (Université de Louvain-la-Neuve, 1978), and references therein.
- <sup>2</sup>F. D. Becchetti, Jr. and G. W. Greenlees, *Phys. Rev.* **182**, 1190 (1969).
- <sup>3</sup>Z. Majka, A. Budzanowski, K. Grotowski, and A. Strzałkowski, *Phys. Rev. C* **18**, 114 (1978).
- <sup>4</sup>J. Albinowski, A. Budzanowski, H. Dabrowski, Z. Rogalska, S. Wiktor, H. Rebel, D. K. Shrivastava, C. Alderliesten, J. Bojowald, W. Oelert, C. Mayer-Böricke, and P. Turek, *Nucl. Phys.* **A445**, 477 (1985).
- <sup>5</sup>P. P. Singh, P. Schwandt, and C. C. Yang, *Phys. Lett.* **59B**, 113 (1975).
- <sup>6</sup>L. W. Put and A. M. J. Paans, *Nucl. Phys.* **A291**, 93 (1977).
- <sup>7</sup>F. G. Perey, *Phys. Rev.* **131**, 745 (1963).
- <sup>8</sup>J. Bojowald, H. Machner, W. Oelert, M. Rogge, and P. Turek, *Nucl. Instrum. Methods A* **253**, 298 (1987), and unpublished.
- <sup>9</sup>P. L. Robertson, D. A. Goldberg, N. S. Wall, L. W. Woo, and H. L. Chen, *Phys. Rev. Lett.* **42**, 54 (1979).
- <sup>10</sup>D. A. Goldberg, S. M. Smith, and G. F. Burdzik, *Phys. Rev. C* **10**, 1362 (1974).
- <sup>11</sup>J. Raynal, optical model code MAGALI, Centre d'Etudes Nu-

- cleaires Report DPh-T/69-42 1969.
- <sup>12</sup>D. A. Goldberg, S. M. Smith, H. G. Pugh, P. G. Roos, and N. S. Wall, *Phys. Rev. C* **7**, 1938 (1973).
- <sup>13</sup>H. H. Chang, B. W. Ridley, T. H. Braid, T. W. Conlon, E. F. Gibson, and N. S. P. King, *Nucl. Phys.* **A270**, 413 (1976).
- <sup>14</sup>C. M. Perey and F. G. Perey, *At. Data Nucl. Data Tables* **17**, 1 (1976), and references therein.
- <sup>15</sup>M. Matoba, M. Hyakutake, and I. Kumabe, *Phys. Rev. C* **32**, 1773 (1985).
- <sup>16</sup>B. Bonin *et al.*, *Nucl. Phys.* **A445**, 381 (1985), and references therein.
- <sup>17</sup>H. Rebel *et al.*, *Nucl. Phys.* **A182**, 145 (1972); H. Rebel *et al.*, *Z. Phys.* **250**, 258 (1972); V. Corcalciuc, *et al.*, *ibid.* **A 305**, 351 (1982); H. J. Gils and H. Rebel, *Phys. Rev. C* **13**, 2159 (1976); Kernforschungszentrum Karlsruhe (KFK) Report 2838, 1979; KFK Report 3378, 1983 (unpublished); and H. Rebel and H. J. Gils (private communication).
- <sup>18</sup>P. D. Kunz, DWUCK IV, computer code for DWBA calculations, University of Colorado, 1969 (unpublished).
- <sup>19</sup>A. Budzanowski *et al.*, *Phys. Rev. C* **17**, 951 (1978), and private communication.
- <sup>20</sup>H. Rebel, R. Löhken, G. W. Schweimer, G. Schatz, and G. Hauser, *Z. Phys.* **256**, 258 (1972).